ENGINEERING RESEARCH INSTITUTE
UNIVERSITY OF MICHIGAN
ANN ARBOR

PERMEABILITY MEASUREMENTS IN MAGNETIC FERRITES

Technical Report No. 9
Electronic Defense Group
Department of Electrical Engineering

By: L. W. Orr

Approved by: H. W. Welch, Jr.

Project M970

TASK ORDER NO. EDG-4
CONTRACT NO. DA-36-039 sc-15358
SIGNAL CORPS, DEPARTMENT OF THE ARMY
DEPARTMENT OF ARMY PROJECT NO. 3-99-04-042
SIGNAL CORPS PROJECT NO. 29-194B-0

September, 1952

TABLE OF CONTENTS

	Page
LIST OF ILLUSTRATIONS	iii
ABSTRACT	iv
ACKNOWLEDGMENT	v
1. INTRODUCTION	1
2. GENERAL REMARKS	3
3. MAGNETIC RADIUS AND APPLIED FIELD	4
4. KINDS OF PERMEABILITY	5
5. TEST CORES	8
6. B-H LOOPS	11
7. μ -H PLOTS	15
8. MU SURFACE	22
9. APPLICATION OF MU SURFACES	23
9.1 Tuning Units	27
9.2 Modulator Units	28
9.3 Flip Flop Units	28
10. BUTTERFLY LOOPS	28
11. INITIAL PERMEABILITY MEASUREMENT	33
12. TEMPERATURE VARIATION OF μ_r	36
13. TIME VARIATION OF μ_o	37
APPENDIX I	42
APPENDIX II	44
DISTRIBUTION LIST	47

LIST OF ILLUSTRATIONS

Fig. No.	Title	Page
1	Variation of Magnetic Radius $\bar{R}$ with Toroidal Radii r and R	6
2	Definitions of Magnetic Parameters	7
3	Diagram of Test Core Showing Windings and Thermocouple	9
4	Ferrite Test Cores and Housing	10
5	B-H Plotting Circuit	12
6	Symmetric B-H Loops for Ferramic H at Zero Bias Field	14
7	Minor B-H Loops for Ferramic H with Varying Bias Field	14
8	μ_Δ vs H_o Positive Values Only	16
9	μ-H Plotting Circuit	17
10	Waveforms in μ-H Circuit	18
11	μ-H Oscillogram for Ferramic I	21
12	Mu Surface for Ferramic G	24
13	Mu Surface for Ferramic H	25
14	Mu Surface for Ferramic I	26
15	μ_Δ vs H_o Positive and Negative Values	30
16	Butterfly Loop Plotting Circuit	31
17	Butterfly Loop Oscillogram for Ferramic G	32
18	μ-H Oscillogram for Ferramic G	32
19	μ_o-Measuring Circuit	34
20	Transitron Oscillator Circuit	38
21	Frequency-Temperature Curves for Ferramic G at Various Bias Fields	39
22	Frequency-Time Curves for Various Materials	41

ABSTRACT

The introduction gives a brief note on the development of magnetic ferrites. Practical laboratory methods of measuring magnetic parameters are outlined with particular attention to various permeability measurements. Incremental permeability is presented as a three dimensional "mu surface," and applications of this are discussed. Sample results on several specimens are presented. The temperature variation of reversible permeability and the time decrease of permeability are given for several materials.

ACKNOWLEDGMENT

The author wishes to thank Mr. A. Van Bronkhorst for his assistance in proofreading and Mr. D. M. Grimes for preparing the mathematical development in Appendix II.

PERMEABILITY MEASUREMENTS IN MAGNETIC FERRITES

1. INTRODUCTION

There has been a constant search over the last century for magnetic materials of high permeability. The demands of the communications field and others have intensified this search to the point of creating a science out of the art of metallurgy, with particular attention to magnetic alloys. The parallel studies of the solid state have indicated that quite interesting magnetic properties should be obtained if one could reduce both the crystal anisotropy constant, K, and the saturation magnetostriction coefficient λ_s to zero. Noting this, various workers[1,2] attempted to form high permeability trinary alloys by first making tri-axial plots of the cruves K = 0 and λ_s = 0 as functions of the composition.[3] In some trinaries these two curves intersected and an alloy of that composition invariably had an unusually large value of μ_o.

The chief difficulty with metallic alloys is their high electrical conductivity, which gives rise to excessive eddy-current loss at high frequencies. A modern class of magnetic material of low conductivity is the ferromagnetic spinel, or ferrospinel structure, commonly termed "ferrite." Synthetic ferrites were first suggested for high frequency applications by Hilpert[4] in 1909. But it

---

[1] Zaimovski, A.S., J. Phys (USSR), 4, p. 563, 1941

[2] Snoek, J.L., New Developments in Ferromagnetic Materials, Elsevier, New York, 1947

[3] See for instance, Bozorth, R.M., Ferromagnetism, p. 100, D. Van Nostrand, New York, 1951

[4] Hilpert, S.,"Magnetic Properties of Ferrites," Ber. Deut. Chem. Ges., 42, pp. 2248-61, 1909

remained for Snoek[1] to apply the technique of $K = 0$, $\lambda_s = 0$ to ferrites of various compositions, thereby obtaining new materials having high permeabilities together with the desired low conductivity.

The saturation magnetization of magnetic ferrites (ca. 5000) is much less than that of iron, and they therefore find use at low inductions. The initial permeability is often 1000 or better, and values up to 4000 have been reported. Specific resistivity is generally in the range 10^4 to 10^9 ohm-cm, so that eddy-current losses are negligible even at high frequencies. The crystal structure of magnetic ferrites is described in the literature.[2,3]

In ferrite single crystals, and other grain oriented magnetic specimens the magnetic parameters vary widely with the direction of measurement.[4] However, the ferrite specimens treated in this report are believed to be polycrystalline and of random orientation, so that their magnetic parameters are independent of the direction of measurement. In samples having internal strain where K and λ_s are not zero, the magnetic parameters are again not exactly independent of the direction of measurement. The variation due to this cause in the specimens measured is not yet known.

The initial permeability of a ferrite rises as the temperature is increased up to a point somewhat below the Curie temperature. Above this point the permeability falls off rather rapidly until the Curie temperature is reached. Since Curie temperature is a function of composition, it is possible to obtain

---

[1]Snoek, J.L., op. cit., p. 1

[2]Harvey, R.L., Hegyi, I.J. and Leverenz, H.W., "Ferromagnetic Spinels for Radio Frequencies," RCA Rev, XI, No. 3, pp. 321-362, Sept. 1950

[3]Bozorth, R.M., Ferromagnetism, p. 244, D. Van Nostrand, New York, 1951

[4]See for instance, Bozorth, R.M., Ferromagnetism, pp. 12, 44

materials with a variety of permeability temperature coefficients within a limited temperature range.[1]

2. GENERAL REMARKS

The variety of methods now used in various technical laboratories to measure magnetic parameters sometimes leads to confusion and misunderstanding.

There is an obvious need for standardizing such methods. It is the hope of the Michigan Group that through this and future reports, a measure of understanding between various organizations can be reached regarding the magnetic parameters of significance, and the choice of techniques to measure them. It is hoped that this understanding will lead to the establishment of standard methods of measurement.

The criterion of a good method is that it be simple, reasonably accurate and easily performed. The equipment involved should be capable of construction with readily available electronic components, and easily duplicated in other laboratories with modest facilities. The methods to be discussed were developed with this in mind.

The determination of magnetization curves, hysteresis loops, and permeabilities depends upon (a) the application of known magnetic fields to the specimen, and (b) the determination of the resulting flux, usually by a sensing winding from which the flux density changes are calculated.

The techniques for performing these measurements vary, depending upon the accuracy required and upon the shape of the specimen. For rod specimens, the most difficult quantity to determine is the field strength because the field

---

[1] See for instance, Harvey, R.L., Hegyi, I.J. and Leverenz, H.W., "Ferromagnetic Spinels for Radio Frequencies," RCA Rev, XI, No. 3, p. 359, Sept. 1950

created by a solenoid wound around the specimen is disturbed by the magnetic poles generated in it. The resulting "demagnetization factor" is a function both of the permeability and of the diameter - length ratio. Several schemes have been devised to overcome this difficulty by closing the magnetic circuit by means of a yoke.

For ring specimens, the demagnetization factor is absent since no salient poles are generated in the specimen, and the applied magnetic field is easily determined. Various ferrites are available in both rod and ring forms as well as a variety of other shapes, however only ring samples were used in the work to be described.

3. MAGNETIC RADIUS AND APPLIED FIELD

For a ring specimen wound with N turns of wire evenly disposed around the toroid, and carrying a current I amperes, the applied field H is given by the equation

$$H = \frac{4\pi NI}{10\ell} = \frac{4\pi NI}{20\pi R} = \frac{NI}{5R} \text{ oersteds} \qquad (1)$$

where R is the toroidal radius in cm, and ℓ is the magnetic path length. If the inner and outer radii, r and R, of the specimen are different, a mean magnetic radius $\bar{R}$ must be found in terms of r and R so that the effective field H is given by

$$H = NI/5\bar{R} \text{ oersteds} \qquad (2)$$

As might be expected, the form of the expression for $\bar{R}$ depends upon the shape of the cross section. Expressions for rectangular and elliptical sectioned

toroids have been derived,[1] and are as follows:

$$\text{Rectangular cross section:} \quad \bar{R} = \frac{R - r}{\log_e R - \log_e r} \tag{3}$$

$$\text{Elliptical cross section:} \quad \bar{R} = \frac{1}{4}\left(\sqrt{R} + \sqrt{r}\right)^2 . \tag{4}$$

Plots of these functions are given in Fig. 1. The ratio $\bar{R}/r$ is plotted against R/r so that the curves may be applied universally. In a particular case, measurements of R and r are made, $\bar{R}$ found from the appropriate curve and the effective field obtained by applying Eq 2.

4. KINDS OF PERMEABILITY

The normal permeability, μ, is generally considered to mean the ratio B/H in a magnetic specimen when it is in the "cylic magnetic state."

The incremental permeability, μ_Δ, refers to the permeability measured with superposed a-c and d-c fields, and indicates the ratio $\Delta B/\Delta H$ when a specimen is cycled around a minor hysteresis loop, such as that shown by path 12341 in Fig. 2. Here we have a d-c bias field H_o with a superposed a-c field of amplitude $1/2\Delta H$. The dashed curve represents the saturation B-H loop for the material.

As ΔH approaches zero, μ_Δ approaches a limiting value of μ_r, the reversible permeability. When the material is demagnetized (B = 0), and no d-c bias is applied ($H_o = 0$), the reversible permeability μ_r becomes μ_o, the initial permeability.

The maximum permeability, μ_m, is the largest possible value of μ_Δ when no bias field is applied ($H_o = 0$). In many ferrites materials μ_Δ reaches the value μ_m for $\Delta H \cong 4H_c$.

[1] See Appendices I and II

FIG. 1
VARIATION OF MAGNETIC RADIUS $\bar{R}$
WITH TOROIDAL RADII r AND R

FIG. 2
DEFINITIONS OF MAGNETIC PARAMETERS

Both μ_Δ and μ_r are dependent on the value of H_o and on the previous magnetic history of the specimen. μ_Δ is also dependent on the size of ΔH as will be shown later.

In most ferrites, when operated well below the Curie temperature, the temperature coefficient of μ_r is positive for low values of H_o and negative for high values of H_o. There is a value of H_o called the crossover field for which $d\mu r/dT = 0$ over a wide temperature range. The crossover field for Ferramic G is ca. 4.5 Oe. from 25°C to 75°C.

5. TEST CORES

For testing magnetic properties, ferrite toroid cores are furnished with H and B windings, and occasionally with a thermocouple,[1] as illustrated in Fig. 3. The H winding is evenly spaced and extends the full 360 degrees around the toroid producing a uniform field, and minimum leakage flux. The B winding, or sensing winding, need not be evenly distributed, but may be lumped in one part of the toroid, because the total flux through any cross section is substantially the same at any instant. However, for the sake of symmetry, the B winding is also a 360 degree distributed winding.

Figure 4 shows typical toroid cores in various stages of assembly. The cores at the top of the picture are shown as furnished from the suppliers. At the lower left is shown a core after applying a 200-turn B winding. At the lower right is shown a core in its housing.

[1]When measuring magnetic parameters in an oven, the voltage at the thermocouple terminals indicates the difference between core temperature and oven temperature. A copper-constantan thermocouple gives 40 millivolts per °C difference in temperature. Since the thermal inertia of the thermocouple is small, it permits readings to be taken before the core comes to thermal equilibrium.

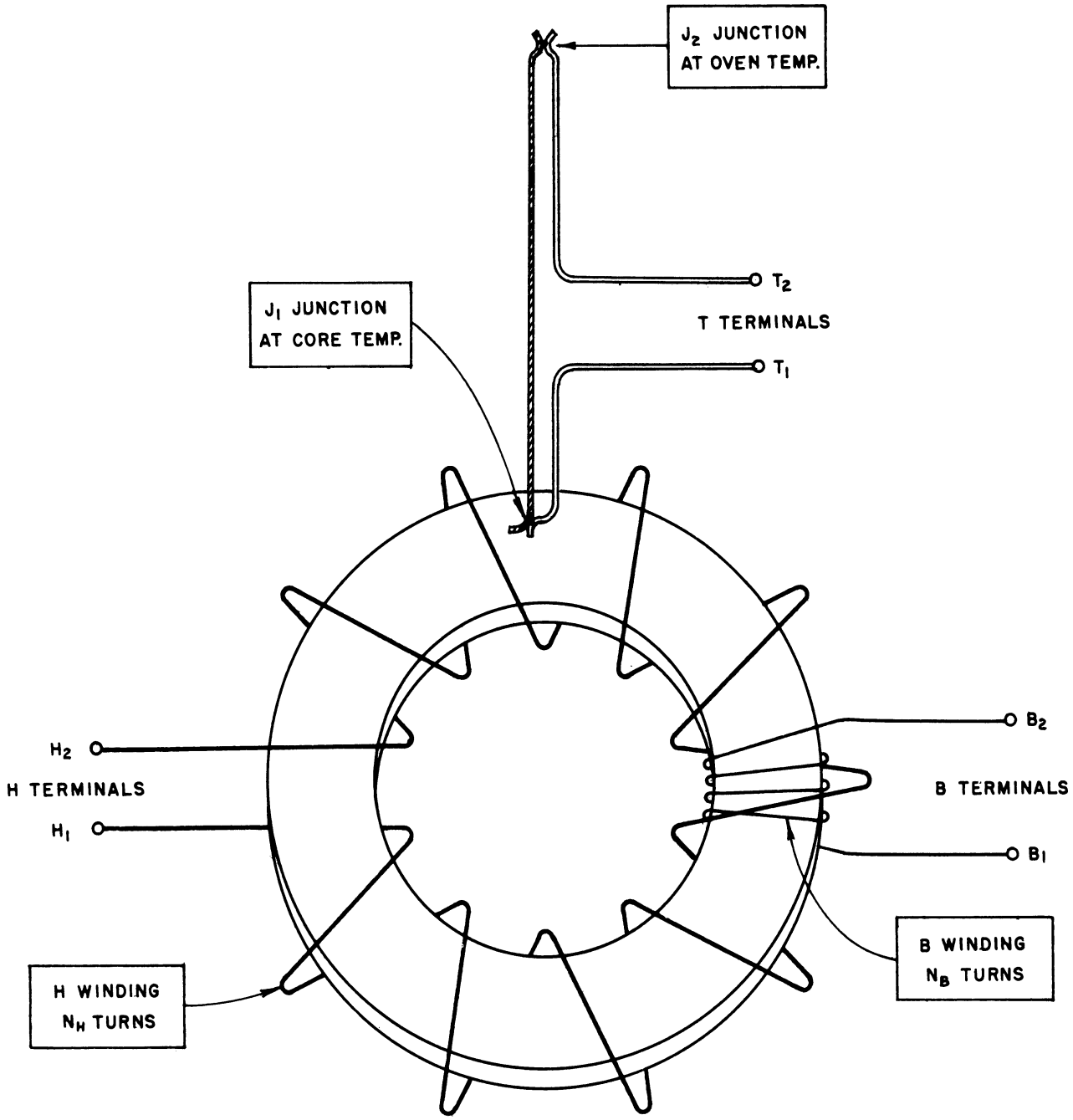

FIG. 3
DIAGRAM OF TEST CORE SHOWING WINDINGS AND THERMOCOUPLE

FIG. 4
FERRITE TEST CORES AND HOUSING

6. B-H LOOPS

Since ferrites are noted for their rather high resistivity, eddy current losses at audio frequencies are negligible. Hence, the B-H loop of a ferrite taken at 1000 cycles will be almost identical with the d-c B-H loop. (As the B-H loop of a material is traced arbitrarily slowly, it approaches a limiting position known as the static B-H loop or d-c B-H loop.)

Oscillograms of 1000 cycle B-H loops may be obtained from test cores using the circuit shown in Fig. 5. In this circuit, an audio oscillator feeds a power amplifier which furnishes the 1000 cycle magnetic field to the core through the H winding. If desired, a d-c bias field may be applied by closing switch S_1 and adjusting the d-c bias control. The bias in oersteds may be found by reading the current I indicated on the meter, and applying Eq 2.

Both a-c and d-c components of current flowing in the H winding also flow in the resistor R_H, forming a voltage drop proportional to the applied field. This voltage is applied to the X input of a d-c coupled oscilloscope, such as a Dumont Mod. 304-H, so that horizontal displacement of the beam is always proportional to the applied field. The X axis of oscillograms may be calibrated in oersteds using the bias circuit described above and Eq 2.

The capacitor C_H is so chosen that its capacitive reactance at oscillator frequency is low compared with other impedances in the H circuit. Thus different values of d-c bias may be applied without affecting the amplitude of the applied a-c field.

Components R_B and C_B form an integrating network which connects the B winding with the Y input of the oscilloscope. The time constant R_BC_B of this network must be several orders of magnitude larger than the period (1/f) of the

FIG. 5
B - H PLOTTING CIRCUIT

oscillator, in order to obtain a faithful B-H display. R_B must also be chosen several orders of magnitude larger than the inductive reactance of the B winding, so that errors due to loading of the B winding will be negligible.

The instantaneous voltage e_1 at terminals B_1, B_2 is given by

$$e_1 = N_B A \frac{dB}{dt} \times 10^{-8} \text{ volts} \qquad (5)$$

where N_B is the number of turns of wire on the B windings, A is the core cross section area in cm^2, and B is the mean flux density in gauss through the area A. If $R_B C_B \gg 1/f$, the voltage e_2 across C_B is given by

$$e_2 \cong \frac{1}{R_B C_B} \int e_1 \, dt = \frac{N_B A B}{R_B C_B} \times 10^{-8} \text{ volts} \qquad (6)$$

and hence

$$B \cong \frac{R_B C_B \times 10^8}{N_B A} e_2 \text{ gauss} \qquad (7)$$

Equation 7 is used in calibrating the B axis of the oscillogram, after a voltage calibration is made.

Figure 6 is an oscillogram showing a series of symmetric B-H loops obtained with the B-H circuit of Fig. 5, and a test core of Ferramic H. The largest loop has a tip induction of 2.76 kga. at a tip field of 1.8 oe. The measured parameters from the oscillogram are as follows:

B_r = 1.76 kga. $\qquad \mu_{max}$ = 3600

B_m = 2.76 kga. $\qquad \mu_o \cong$ 830 (estimated)

H_c = 0.25 oe.

These values approximate the data furnished by the supplier.

FIG. 6

SYMMETRIC B - H LOOPS FOR FERRAMIC H AT ZERO BIAS FIELD

FIG. 7

MINOR B - H LOOPS FOR FERRAMIC H WITH VARYING BIAS FIELD

It is possible to display minor hysteresis loops at various values of d-c bias field, H_o. Oscillograms of such loops are shown in Fig. 7. From left to right the loops are for H_o = 0, 0.25, 0.50, 0.75, 1.00 and 1.25 oe. The specimen is a core of Ferramic H.

If the tips of a minor hysteresis loop are joined by a straight line, its slope is the incremental permeability, μ_Δ. If such lines are drawn on the loops of Fig. 7 their slopes, being measures of μ_Δ, indicate the variation with H_o. From this figure, six points could be plotted on a μ_Δ - H_o curve.

7. μ - H PLOTS

A plot of incremental permeability μ_Δ as a function of uni-directional bias field H_o is shown in Fig. 8. The plot shows that μ_Δ is double valued, being generally larger for an increasing bias field than for a decreasing one. In addition, the value of μ_Δ is also a function of ΔB, the magnitude of the AC field.

Continuous plots of this type may be obtained from oscillograms made with the circuit shown in Fig. 9. A free-running, symmetric multivibrator, VT1, having a period of approximately one second, drives the relay open and closed. Capacitor C_4 is thus alternately charged and discharged, generating a sawtooth voltage which varies between ca. -50 volts and -5 volts (Fig.10A) when resistors R_{15} and R_{16} are suitably adjusted. This sawtooth voltage, applied to the control grid of VT2, produces a d-c plate current variation (Fig. 10B) from substantially zero (cut-off), to a maximum of ca. 150 milliamperes, furnishing a slowly varying bias field, H_o.

It is noted that this current variation is quite non-uniform, but this is no disadvantage, and there are two distinct advantages:

FIG. 8

μ_Δ VS. H_0
POSITIVE VALUES ONLY

FIG. 9

μ-H PLOTTING CIRCUIT

A GRID VOLTAGE OF VT 2

B PLATE CURRENT OF VT 2

FIG. 10

WAVEFORMS IN μ - H CIRCUIT

a. It produces a fairly uniform rate of change of magnetic flux which is sufficiently slow at all points so that the resulting emf induced in the B winding is negligibly small.

b. It produces a horizontal oscilloscope sweep which is slow near zero current and rapid near the extreme. This is very helpful in photographing the oscillogram, for the a-c envelope has a large vertical dimension near $H_o = 0$ requiring a longer exposure for proper density on the film.

The plate current of VT2 is passed in series through the H winding, the milliameter MA and resistor R_4. The horizontal displacement of the beam is proportional to the voltage across R_4 and hence to the bias field H_o. An oscilloscope with d-c coupled amplifiers (such as the Dumont 304-H) is used to avoid low frequency phase shift.

To furnish the μ-measuring signal, a sine-wave audio oscillator is connected to the B winding in series with resistors R_2 and R_3. It is found convenient to work the oscillator at a frequency between 1 kc and 10 kc. The actual frequency is not important, since it does not enter the calculations. ΔH may be varied by adjusting either the oscillator gain or R_2. It is desirable to have R_2 large compared to the maximum impedance of the B winding so that the a-c current in this winding is sinusoidal and of constant amplitude despite winding impedance variations. It is also desired to keep the a-c impedance of the H_o circuit large to prevent excessive loading of the H winding. This is accomplished by the large plate resistance of VT2 (ca. 40,000 ohms) in series with the H winding.

The value of ΔH is found by reading the r.m.s. voltage drop e_3 across the standard 10 ohm resistor R_3 with a vacuum tube voltmeter (such as the Hewlett-Packard Mod. 400 C). The quantity ΔB is found by means of the integrating circuit R_1C_1 connected across the B winding. The vertical dimension of the

oscillogram is a measure of ΔB, and thus proportional to μ_Δ for a fixed ΔH. The values of R_1 and C_1 are chosen to minimize the loading on the B winding, and to have a time constant $R_1 C_1$ such that

$$\frac{1}{f} \ll R_1 C_1 \ll T$$

where f is the oscillator frequency, and T is the period of the multivibrator VT1. An electrostatic shield surrounds the integrator circuit preventing the pickup of stray fields.

A typical oscillogram, Fig. 11, indicates for Ferramic I the variation of μ_Δ over a range $0 \leqslant H_o \leqslant 1.4$ oe. The horizontal calibration is 0.05 oe. per small square. The value of ΔH is 0.74 oe. (peak to peak). The two horizontal streaks have a vertical separation of $\mu_\Delta = 1200$.

Oscillograms are easily made with the Land Polaroid Camera, and an exposure of several seconds at F:5.6 or F:8. They are reduced to plots such as Fig. 8 by voltage calibrating the horizontal and vertical axes, and employing the following calibration equations.

Horizontal $$H_o = \frac{N_H e_H}{5\bar{R}\, R_4} \quad \text{oersteds} \tag{8}$$

Vertical $$\Delta B = \frac{10^8\, R_1 C_1 e_V}{A N_B} \quad \text{gauss} \tag{9}$$

$$\Delta H = \frac{2\sqrt{2}\; N_B e_3}{5\bar{R}\, R_3} \quad \text{oersteds} \tag{10}$$

$$\mu_\Delta = \frac{\Delta B}{\Delta H} \tag{11}$$

FIG. 11

μ - H OSCILLOGRAM FOR FERRAMIC I

where

A = core cross section area (cm^2)

ΔB = range of flux-density change (gauss) produced by ΔH

e_3 = indicated r.m.s. voltage across R_3 (volts)

e_H = horizontal dimension on oscillogram (volts)

e_V = vertical dimension on oscillogram (volts)

H_o = d-c bias field (oersteds)

ΔH = range of a-c field (oersteds)

N_B = number of turns on B winding

N_H = number of turns on H winding

$\bar{R}$ = *mean magnetic radius (cm)

R_1C_1 = time constant of integrator (sec)

R_3 = ΔH - measuring resistor (ohms)

R_4 = H_o - measuring resistor (ohms)

8. MU SURFACES

It is of particular interest in many applications to present the incremental permeability μ_Δ as a function of the two variables H_o and H. This can conveniently be done by a three-dimensional solid, the curved surface of which represents the function μ_Δ. It is convenient to present this solid in isometric projection, in which the axes of μ_Δ, H_o and ΔH intersect at 120°. The mu surface is described by drawing the projected curves of intersection when it is sliced by two perpendicular sets of vertical planes which are parallel to the planes $H_o = 0$ and $\Delta H = 0$ respectively.

*See Eqs 3 and 4, p. 5

Since each slice for a plane of constant ΔH will have the double-valued form of Fig. 8, the surface also will be double-valued except at $H_o = 0$ and $H_o = H_{max}$. To avoid confusion, only the upper branch of the mu surface will be presented here (i.e., the surface for H_o increasing).

Figures 12, 13 and 14 show the upper mu surfaces obtained for Ferramics G, H and I. Each projection was plotted from a set of properly calibrated oscillograms made with the Land Polaroid Camera and the circuit in Fig. 9.

Since no oscillogram is possible when $\Delta H = 0$, the curve in the $\Delta H = 0$ plane is obtained by extrapolation, and is shown as a dashed curve in the figures.

A study of mu surfaces gives a new insight into the magnetic properties of these materials and their specific applications. It is seen that the permeability changes rapidly with ΔH for small values of H_o but only slowly for large values of H_o. To understand this effect, it is helpful to refer to Fig. 2. Here the dashed curve shows the saturation B-H loop and represents the outer limits of the magnetic condition of the core. When H_o is large, the minor hysteresis loop is drastically confined by the branches of the dashed curve, and therefore its slope (μ_Δ) cannot change much with a variation in the size of ΔH.

The intercept of the mu surface at the origin is denoted by μ_o', the reversible permeability at $H_o = 0$, $B = B_r$. This is not to be confused with the initial permeability μ_o, which in ferrites is larger than μ_o'. A method of measuring μ_o is described in Section 11.

9. APPLICATION OF MU SURFACES

Many magnetic applications are greatly facilitated by the use of mu surfaces, and three examples are given as illustrations.

FIG. 12
MU SURFACE FOR FERRAMIC G

FIG. 13
MU SURFACE FOR FERRAMIC H

M-970 C-64-21 RKL 4-28-52

FIG. 14
MU SURFACE FOR FERRAMIC I

9.1 Tuning Units

Magnetic tuning units are of particular interest in radio receivers where electronic tuning is desired. Such units are ideally constructed of ferrite materials because of the low losses at high frequencies and the remarkable ability to change the incremental permeability, and hence the inductance of the unit, by applying a current to the control winding which produces a varying bias field.

It is of primary interest to know the range of permeability for a particular material under various ranges of bias field. It is desirable, for instance, that the control field requirements be small for a given change of permeability. Such information is adequately given by a curve such as Fig. 8 drawn for a quite small r-f field, as would normally exist in the r-f stages of a receiver.

In a superheterodyne circuit it is necessary to vary the local oscillator unit so that it tracks with the r-f unit. For most oscillators of variable frequency in which the frequency variation is obtained by changing the inductive element, the circulating current in the tank, and hence the value of ΔH in the core of the inductor, will vary with frequency.

A permeability curve of constant ΔH, such as Fig. 8, is no longer useful for engineering design purposes, since one must examine the manner in which the permeability changes when both H and ΔH vary as dictated by the circuit.

The mu surface for a particular material permits this type of analysis to be made without constructing a test unit. A laborious trial and error solution is thus avoided. One can see the variations of incremental permeability of a proposed tuning unit by tracing the curve of H vs ΔH over the mu surface. An estimate of the tracking error may be made by such an analysis and certain materials may be discarded at once as unfavorable by inspection.

9.2 Modulator Units

For a magnetic modulator[1] of maximum sensitivity, the maximum value of $d\ \mu_\Delta/dH_o$ is desired. This will produce the largest unbalance signal for a given change in control field H_o. The mu surfaces not only indicate the best materials for this criterion, but give the optimum values of H_o and ΔH for a particular materials.

An examination of the three surfaces presented in Figs. 12, 13 and 14 shows that Ferramic I is the best of the three for this, even though its maximum permeability (2,900) is less than that of Ferramic H (3,700). By interpolation from Fig. 14 one obtains for Ferramic I

$$\left[\frac{d\,\mu_\Delta}{dH_o}\right]_{max} = 12{,}700 \text{ per oersted,}$$

at $H_o = .05$ oe. and $\Delta H = .37$ oe.

9.3 Flip Flop Units

For a dynamic magnetic flip flop,[2] one criterion is that a large total change of μ_Δ be produced by varying ΔH. An associated criterion is that $d\,\mu_\Delta/d(\Delta H)$ be a maximum for most rapid transition from low current to high current conditions. These criteria are easily checked for various materials from their mu surfaces. An examination of Figs. 12, 13 and 14 shows that Ferramic H is the preferred material of the three, and should be operated at zero bias ($H_o = 0$) in this application.

10. BUTTERFLY LOOPS

If incremental permeability is plotted against bias field H_o as the latter is cycled alternately through positive and negative values, one obtains

[1] See for instance, Wennerberg, "A Simple Magnetic Modulator for Conversion of Millivolt D-C Signals," AIEE Conference, Pasadena, California, June, 1951

[2] See for instance, Isborn, Carl, "The Ferro-Resonant Flip Flop," IRE Convention, New York, March, 1952

the familiar butterfly loop[1] as illustrated in Fig. 15. The circuit of Fig. 9 may be modified to display such loops by installing a reversing relay in the H_o circuit. This relay must operate so that the H_o circuit is reversed each time the current in VT2 reaches its minimum value (substantially zero).

The modified circuit for performing this operation is shown in Fig. 16. Here relay 2 is the reversing relay, and is actuated by a flip-flop tube VT3 having two stable states. Since the relay must reverse at the time of minimum current in VT2, or when the voltage on capacitor C_4 is most negative, it must operate at the time relay 1 closes. At this time, the left-hand plate of VT1 goes into conduction, and its voltage drops suddenly.

When this plate-voltage drop is differentiated by the network C_6R_{20}, a negative pulse is formed which is applied to the grids of VT3 through diode D1 and capacitors C_9 and C_{10}. The negative pulse upsets VT3 and relay 2 reverses. Diode D1 prevents positive pulses from being applied to the grids of VT3, so that the flip-flop VT3 is upset only at the proper times.

When relay 2 closes, a small switching transient sometimes produces a random pulse in the B winding, smearing the oscillogram slightly at $H_o = 0$. This difficulty can be overcome by arc-suppressing capacitors across the contacts of relay 2, but these produce capacitive loading of the H winding which is reflected by transformer action into the μ-measuring circuit, causing somewhat erroneous results.

A typical butterfly loop obtained with this circuit for Ferramic G is shown in Fig. 17. Figure 18 shows the corresponding uni-directional H_o oscillogram for the same core and conditions as in Fig. 17. (The circuit is easily restored to its original uni-directional operation either by opening the cathode

[1]Note: A similar loop for 45 Permalloy appears in Bozorth, R.M., Ferromagnetism, p. 542, but the direction of the arrows on the solid curve is incorrect.

FIG. 15

μ_Δ VS. H_0

POSITIVE AND NEGATIVE VALUES

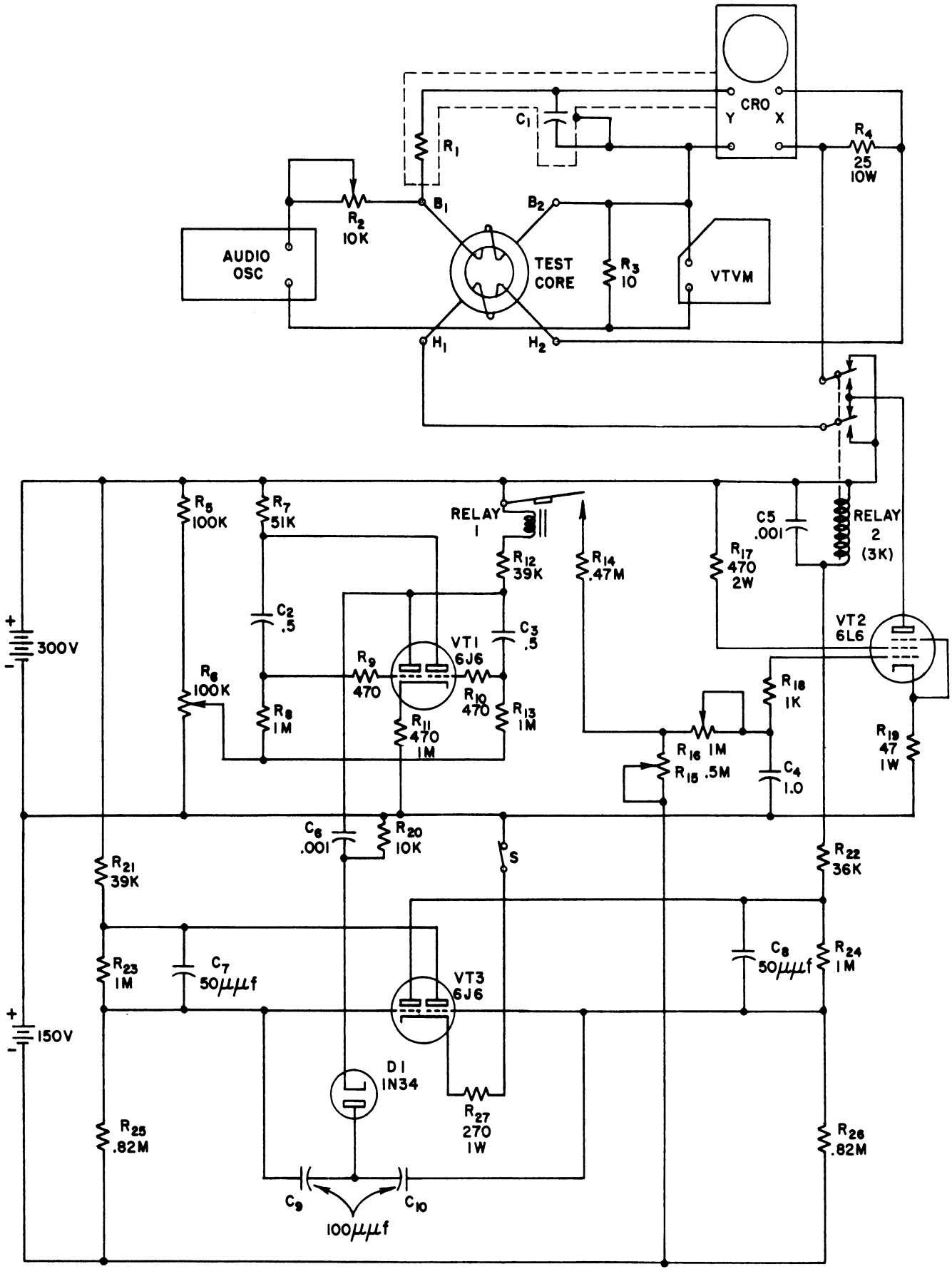

FIG. 16
BUTTERFLY LOOP PLOTTING CIRCUIT

FIG. 17

BUTTERFLY LOOP OSCILLOGRAM FOR FERRAMIC G

FIG. 18

μ-H OSCILLOGRAM FOR FERRAMIC G

circuit of VT3 with switch S, or by removing tube VT3 from its socket.) Calibration of butterfly loop oscillograms is done by employing Eqs 8 to 11 (incl.) as before. The shape of the butterfly loop is again a function of ΔH. The limiting position of the loop as $\Delta H \rightarrow 0$ is a plot of μ_r vs H_o. Some authors apply the term butterfly loop to this plot only. The maximum value of μ_r in such a loop is never greater than μ_o, and is obtained at a bias field equal to the coercive force H_c.

11. INITIAL PERMEABILITY MEASUREMENT

A simple and accurate method of measuring the low frequency initial permeability μ_o of homogeneous toroids of uniform cross section will now be described. The precision is limited only by the precision of a standard resistance box and the precision of maintaining a given audio frequency. (It is assumed that the core dimensions may be measured to any desired degree of precision.)

The circuit employed is very simple, and is shown in Fig. 19. An audio oscillator of sinusoidal waveform and known frequency ω is used in conjunction with a high impedance R_1 to furnish a sinusoidal current. This current is passed in series through the N-turn winding on the toroid to be measured and the standard resistance box R_2.

In position 1, the reversing switch S permits measurement of the voltage drop across the coil, while in position 2 it permits measurement of the voltage drop in R_2. In either position, the vacuum-tube voltmeter and oscillator remain grounded. R_2 is adjusted so that the two readings on the meter are identical.

FIG. 19

μ_0 - MEASURING CIRCUIT

When the reversing switch S is in position 1, the input capacitance of the meter is across the coil. It is important to know the resonant frequency $\omega_o = (LC)^{-1/2}$ where L is the inductance of the coil, and C is the sum of the meter, coil and stray capacitances. If the oscillator frequency $\omega \ll \omega_o$, errors due to resonant effects will be avoided.

If the sinusoidal current is small, the flux density may be assumed to be sinusoidal and in phase with the current so that

$$B = \frac{\Delta B}{2} \sin \omega t \quad \text{gauss} . \tag{12}$$

The r.m.s. voltage generated across the N turn winding (indicated by meter in switch position 1) will be

$$E_1 = \frac{NA\ \Delta B\ \omega}{2\sqrt{2} \times 10^8} \quad \text{volts.} \tag{13}$$

Thus

$$\Delta B = \frac{2\sqrt{2}\ E_1\ 10^8}{\omega NA} \quad \text{gauss.} \tag{14}$$

The applied field caused by a peak current I_{max} has amplitude $1/2\Delta H$ so that

$$\Delta H = \frac{2NI_{max}}{5\bar{R}} = \frac{2N}{5\bar{R}} \cdot \frac{\sqrt{2}\ E_2}{R_2} \quad \text{oersted.} \tag{15}$$

Where E_2 is the r.m.s. voltage across R_2 (indicated by meter in switch position 2).

The incremental permeability is thus

$$\mu_\Delta = \frac{\Delta B}{\Delta H} = \frac{E_1}{E_2} \cdot \frac{5\bar{R}\ R_2}{\omega A\ N^2}\ 10^8 . \tag{16}$$

When the two voltages are equalized

$$\mu_\Delta = \frac{5\bar{R}\, R_2}{\omega A\, N^2}\, 10^8. \qquad (17)$$

As the signal level is reduced by reducing the oscillator gain, R_2 will approach a limiting value of R_o. The initial permeability is then found from the equation

$$\mu_o = \frac{5\bar{R}\, R_o}{\omega A\, N^2}\, 10^8. \qquad (18)$$

In applying the method, the following steps are taken.

1. Demagnetize[1] the core.
2. Disconnect the demagnetizing circuit completely.
3. Apply a signal to the core as shown in the circuit.
4. Adjust R_2 for $E_1 = E_2$.
5. Make successive reductions in signal amplitude and repeat 4.
6. Find R_o, the limiting value of R_2, and apply Eq 18.

The earth's magnetic field will affect the measurement of μ_o in certain materials depending upon their shape, size and magnetic properties. It may therefore be necessary to work the core within a magnetic shield to make an accurate measurement of μ_o.

12. TEMPERATURE VARIATION OF μ_r

The reversible permeability of most ferrites operated well below their Curie temperature has a positive temperature coefficient for low values of H_o,

[1] The core may be demagnetized by either
a. applying a slowly decreasing 60 cycle field of initial value above saturation and final value zero; or
b. raising the core above its Curie temperature, and cooling slowly to the desired temperature

and a negative coefficient for high values of H_o. At some value of H_o called the crossover field, the temperature coefficient is approximately zero over a wide temperature range.

Since the inductance L of the winding on a magnetic toroid varies directly as its permeability, the resonant frequency $f = 1/2\pi\sqrt{LC}$ of an oscillator tank circuit containing the toroid will represent the permeability variations. An increase in μ produces a decrease in f.

A transitron oscillator circuit for examining such frequency variations is shown in Fig. 20. A very small circulating current is used in the tank circuit so that the variation of μ_r will be represented. Frequencies may be measured with a calibrated communications receiver of suitable frequency range.

The resonant frequency[1] at room temperature (25°C) is denoted as f_o and the ratio f/f_o is plotted for various values of bias field H_o and for different temperatures. The results on Ferramic G are illustrated in Fig. 21. It is seen that the crossover field for Ferramic G is about 4.5 oe. from 25°C to 80°C, and about 3.0 oe. from 75°C to 100°C. Thus the crossover field decreases as the temperature is increased.

It is noted that the temperature coefficient of frequency is rather large and positive above 100°C at H_o = 6 oe. This indicates that the value of $d\mu_r/dT$ is strongly negative under these conditions.

13. TIME VARIATION OF μ_o

Some types of ferrites after receiving a demagnetization treatment and then left alone at room temperature, suffer from a slow decrease in initial

[1]The frequencies employed ranged from 0.2 mc to 5 mc

FIG. 20
TRANSITRON OSCILLATOR CIRCUIT

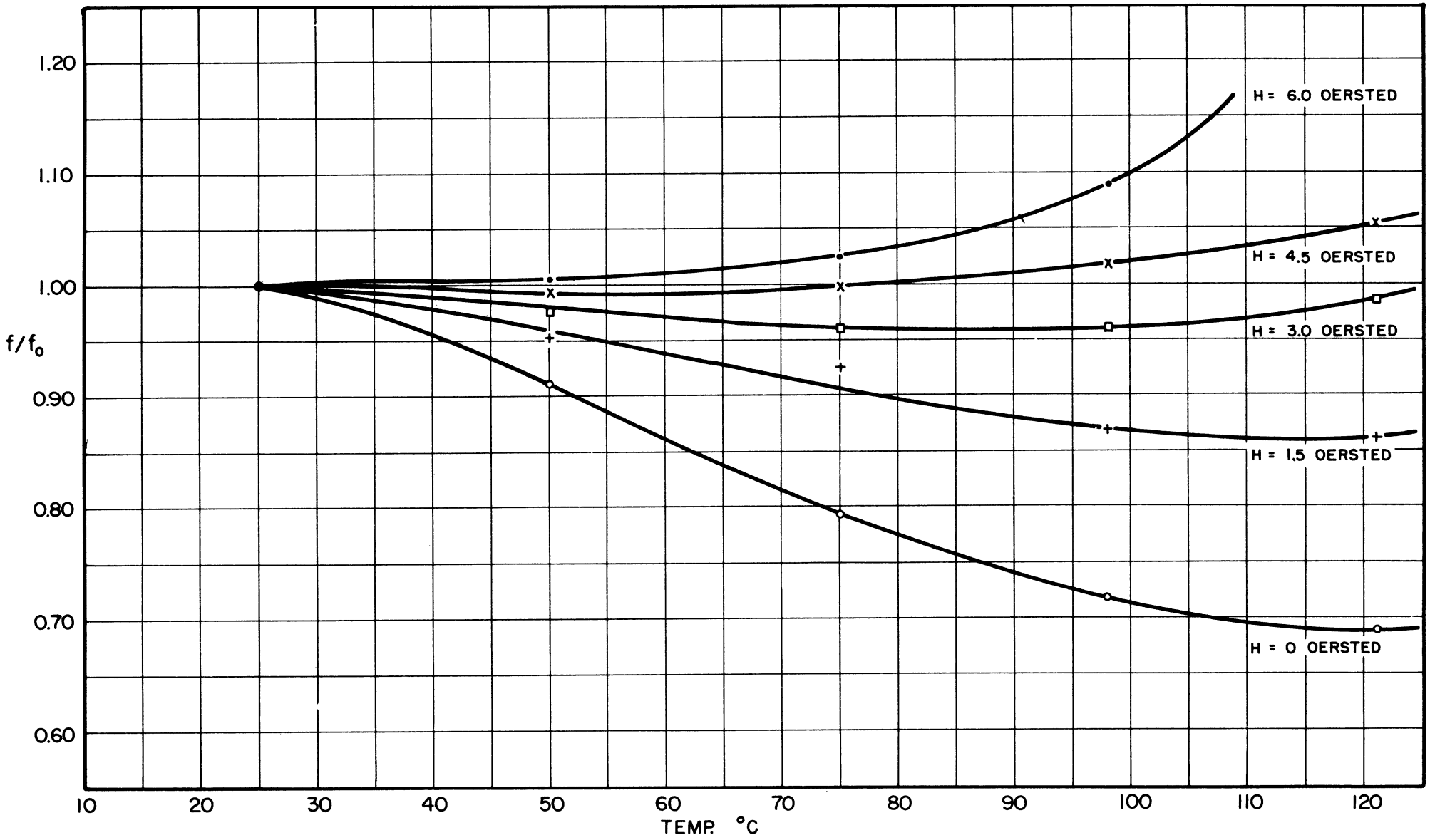

FIG. 21

FREQUENCY - TEMPERATURE CURVES FOR FERRAMIC G AT VARIOUS BIAS FIELDS

permeability. The effect may be observed by noting the resonant frequency over a period of time using a test core in the oscillator circuit of Fig. 20. The oscillator is left on continuously, but the core is inserted only long enough to permit a reading to be taken. Approximately[1] twice the per cent rise in the resonant frequency indicates the per cent decrease in μ_o.

This effect is mentioned by Snoek[2] and was found to appear only in certain materials. It was not observed in Ferramic B or Ferramic I. The frequency drift in several other materials is illustrated in Fig. 22. Ferramic G shows the largest effect, and appears to take longest (ca. 20 hours) to come to equilibrium.

[1]The actual relation between $\Delta\mu/\mu_o$ and $\Delta f/f_o$ is given by the series

$$\frac{\Delta\mu}{\mu_o} = -2\frac{\Delta f}{f_o} + 3\left(\frac{\Delta f}{f_o}\right)^2 - 4\left(\frac{\Delta f}{f_o}\right)^3 + - \ldots$$

For example, a 4% rise in frequency represents a 7.5% decrease in permeability.

[2]Snoek, op. cit., p. 1

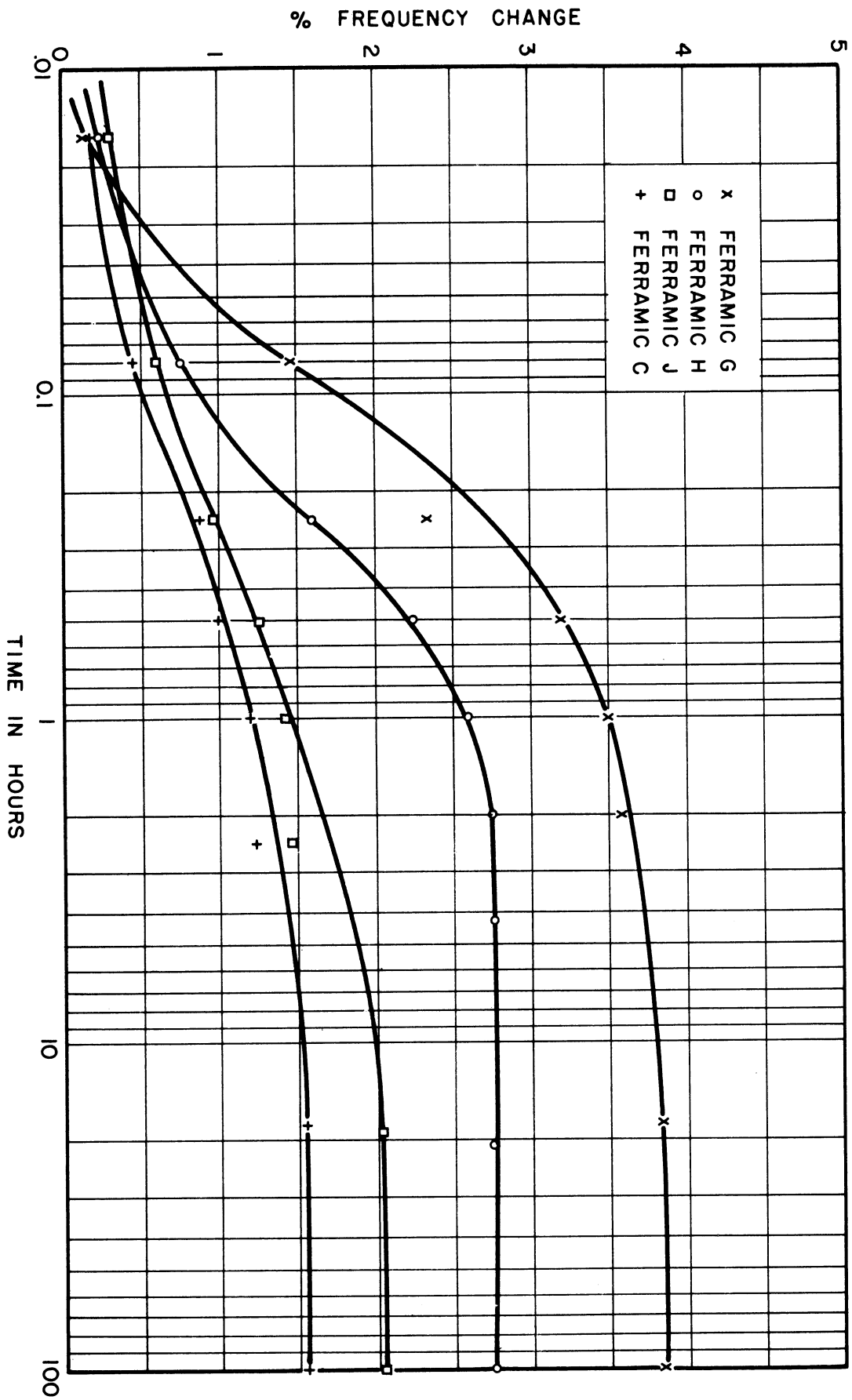

FIG. 22

FREQUENCY-TIME CURVES FOR VARIOUS MATERIALS

APPENDIX I

Mean Magnetic Radius of Toroid of Uniform Rectangular Cross Section

It is desired to find $\bar{R}$ for the toroid such that the average field

$$H = \frac{1}{A} \int_A \mathcal{H}\, dA \qquad (19)$$

is given by

$$H = \frac{NI}{5\bar{R}} \text{ oersteds.} \qquad (20)$$

For a rectangular cross section,

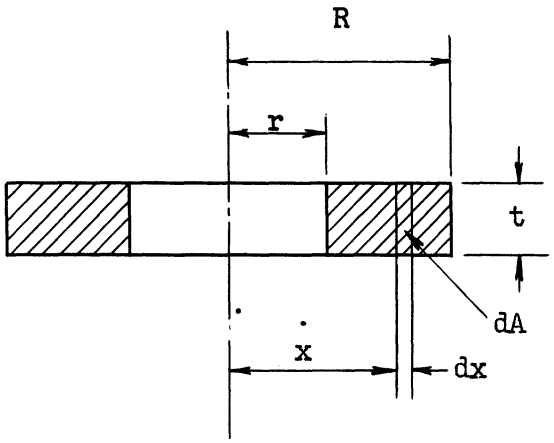

$$dA = t\,dx$$

$$A = t \int_r^R dx$$

$$= t(R - r)$$

The field in the element dA of radius X is given by

$$\mathcal{H} = \frac{NI}{5x} . \qquad (21)$$

Hence the average field from Eq 19 is

$$H = \frac{NI}{5} \cdot \frac{1}{t(R-r)} \int_r^R \frac{t}{x}\, dx$$

$$= \frac{NI}{5} \cdot \frac{\log_e R - \log_e r}{R - r} \qquad (22)$$

And the value of $\overline{R}$ to be used in Eq 20 is therefore

$$\overline{R} = \frac{R - r}{\log_e R - \log_e r} \tag{23}$$

for a rectangular cross section.

APPENDIX II

Mean Magnetic Radius of Toroid of Uniform Elliptical Cross Section

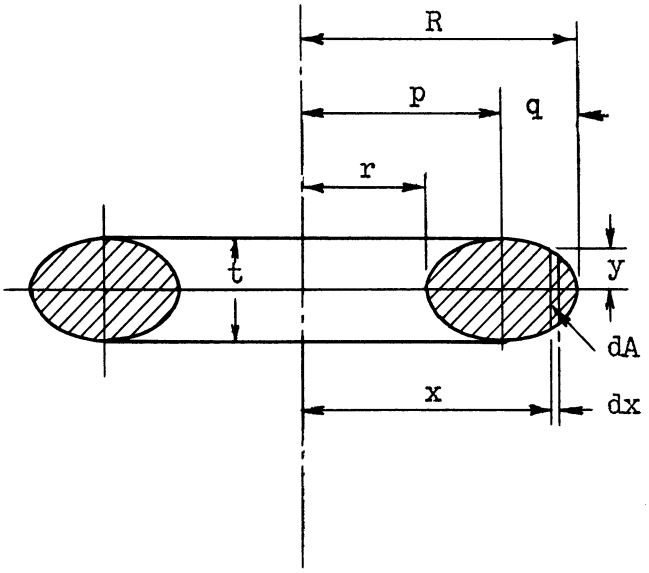

The toroid has inner and outer radii r and R, and thickness t.

Let $p = \frac{1}{2}(R + r)$

and $q = \frac{1}{2}(R - r)$

The ordinate y will be given for an elliptic section by the equation

$$y = k \left[q^2 - (x - p)^2\right]^{\frac{1}{2}} \tag{23}$$

where

$$k = \frac{t}{2q} .$$

The element of area

$$dA = 2y\,dx = 2k \left[q^2 - (x - p)^2\right]^{\frac{1}{2}} dx \tag{24}$$

and the section area

$$A = \int_r^R dA = 2k \int_{p-q}^{p+q} \left[q^2 - (x - p)^2\right]^{\frac{1}{2}} dx \tag{25}$$

This integral is equal to

$$A = 2k \int_{-q}^{q} (q^2 - x^2)^{\frac{1}{2}} \, dx$$

$$= k \left[x(q^2 - x^2)^{\frac{1}{2}} + q^2 \sin^{-1} \left(\frac{x}{q}\right) \right]_{-q}^{q}$$

$$= k \, q^2 \pi \quad . \tag{26}$$

It is desired to find $\bar{R}$ such that the average field

$$H = \frac{1}{A} \int_A \mathcal{H} \, dA \tag{19}$$

is given by

$$H = \frac{NI}{5\bar{R}} \tag{20}$$

Substituting Eqs 21, 24 and 26 in Eq 19 and simplifying, we obtain

$$H = \frac{2NI}{5q^2\pi} \int_{p-q}^{p+q} \frac{\sqrt{q^2 - (x - p)^2}}{x} \, dx \tag{27}$$

To solve this integral, we shall let

$$x - p = q \cos \theta$$

$$dx = - q \sin \theta \, d\theta$$

and $$\left[q^2 - (x - p)^2\right]^{\frac{1}{2}} = q \sin \theta \, .$$

Substituting these in Eq 27, we obtain

$$H = -\frac{2NI}{5q^2\pi} \int_{-\pi}^{o} \frac{q^2 \sin^2\theta \, d\theta}{q\cos\theta + p}$$

$$= \frac{2NI}{5q^2\pi} \left[-q \int_{-\pi}^{o} \cos\theta \, d\theta + q \int_{-\pi}^{o} \frac{q + p\cos\theta}{q\cos\theta + p} \, d\theta \right]$$

The first integral in the bracket is zero. The second integral may be separated to give

$$H = \frac{2NI}{5q^2\pi} \left[p \int_{-\pi}^{o} d\theta - (p^2 - q^2) \int_{-\pi}^{o} \frac{d\theta}{q\cos\theta + p} \right].$$

This may be integrated by Pierce's Tables No. 300 giving

$$H = \frac{2NI}{5\pi q^2} \left[p\theta - 2\sqrt{p^2 - q^2} \tan^{-1} \left(\frac{p^2 - q^2}{p + q} \tan\tfrac{1}{2}\theta \right) \right]_{-\pi}^{o}$$

$$= \frac{2NI}{5\pi q^2} \left(p - \sqrt{p^2 - q^2} \right) \qquad (28)$$

Eliminating H from Eqs 20 and 28, and substituting for p and q, we have

$$\bar{R} = \frac{q^2}{2\left(p - \sqrt{p^2 - q^2}\right)}$$

$$= \frac{(R - r)^2}{4\left(R + r - 2\sqrt{Rr}\right)}$$

$$= \tfrac{1}{4}\left(\sqrt{R} + \sqrt{r}\right)^2, \qquad (29)$$

the mean magnetic radius for a toroid of uniform elliptical cross section.

DISTRIBUTION LIST

1 copy	M. Keiser Chief, Countermeasures Branch Evans Signal Laboratory Belmar, New Jersey
75 copies	Transportation Officer, SCEL Evans Signal Laboratory Building No. 42 Belmar, New Jersey FOR - Signal Property Officer Inspect at Destination File No. 25052-PH-51-91(1443)
1 copy	W. G. Dow Prof., Dept. of Electrical Engineering University of Michigan Ann Arbor, Michigan
1 copy	H. W. Welch, Jr. Engineering Research Institute University of Michigan Ann Arbor, Michigan
1 copy	Document Room Willow Run Research Center University of Michigan Ann Arbor, Michigan
10 copies	Electronic Defense Group Project File University of Michigan Ann Arbor, Michigan
1 copy	Engineering Research Institute Project File University of Michigan Ann Arbor, Michigan